

Article

# Distribution of Concentrated Loads in Timber-Concrete Composite Floors: Simplified Approach

Sandra Monteiro <sup>1,\*</sup>, Alfredo Dias <sup>1</sup> and Sérgio Lopes <sup>2</sup>

<sup>1</sup> The Institute for Sustainability and Innovation in Structural Engineering, Civil Engineering Department, University of Coimbra, Rua Luís Reis Santos—Pólo II, 3030-788 Coimbra, Portugal; alfgdias@dec.uc.pt

<sup>2</sup> Centre for Mechanical Engineering, Materials and Processes, Civil Engineering Department, University of Coimbra, Rua Luís Reis Santos—Pólo II, 3030-788 Coimbra, Portugal; sergio@dec.uc.pt

\* Correspondence: sandra@dec.uc.pt

Received: 30 December 2019; Accepted: 13 February 2020; Published: 18 February 2020



**Abstract:** Timber-concrete composite (TCC) solutions are not a novelty. They were scientifically referred to at the beginning of the 20th century and they have proven their value in recent decades. Regarding a TCC floor at the design stage, there are some assumptions, at the standard level, concerning the action of concentrated loads which may be far from reality, specifically those associating the entire load to the beam over which it is applied. This naturally oversizes the beam and affects how the load is distributed transversally, affecting the TCC solution economically and mechanically. Efforts have been made to clarify how concentrated loads are distributed, in the transverse direction, on TCC floors. Real-scale floor specimens were produced and tested subjected to concentrated (point and line) loads. Moreover, a Finite Element (FE)-based model was developed and validated and the results were collected. These results show that the “loaded beam” can receive less than 50% of the concentrated point load (when concerning the inner beams of a medium-span floor, 4.00 m). Aiming at reproducing these findings on the design of these floors, a simplified equation to predict the percentage of load received by each beam as a function of the floor span, the transversal position of the beam, and the thickness of the concrete layer was suggested.

**Keywords:** TCC floors; transverse distribution of load; concentrated loads; simplified approach

## 1. Introduction

Since its first scientific reference in the early decades of the last century [1], the use of a composite solution gathering timber beams with a thin concrete layer through an efficient connection has been spreading either for new or rehabilitation applications, on building floors or on bridge decks [2]. Timber-concrete composite (TCC) solutions may be as versatile as needed, by using different materials: different concrete strengths or densities, different timber species or engineered products, and different connection systems; or different sections (thicknesses and shape) [3–8]. They were initially developed with the aim of rehabilitating or strengthening timber floors [9]. However, in some cases of heritage cultural value buildings, their use may be overlooked by their insufficient reversibility [10] or for being a non-dry technique. In fact, there are cases where TCC solutions were preferred relatively to other rehabilitation techniques and were also recognized as prize-worthy [11–13].

The rehabilitation of a building floor may be a consequence of physical or biological damages, lack of strength for the associated use (actual or new one), among others. Regardless of the motivation, there are common types of loading, such as furniture (point loads) or partition walls (line loads) that must be considered at the design stage. Concerning a timber-concrete solution, beside a document that is being prepared [14], there are no current standardization or code rules for the design for such composites. Annex B of the Eurocode 5 [15] is commonly used to perform the design computation.

This computation considers the association of the entire load, point or line load aligned with the length of the timber beam, with the beam under consideration, but it can be far from the real behavior. In recent years, a few studies [16–21] aiming to understand how the load is distributed in the transverse direction were performed in this field. Parameters that might affect that distribution were investigated. The work developed by the authors [16–18] proves that the share of load received by the loaded beam could be, in some cases, less than half. It is easy to understand the economic implications that an overestimated cross-section may have, associated with the unnecessary waste of material. Furthermore, there are also consequences at the mechanical behavior level. The thicker the concrete slab (using the same timber cross-section), the higher the transverse distribution of load. The opposite occurs with the increase of the timber beam height (keeping the concrete thickness unchanged), but with less expression [22], hence the importance of such studies.

This paper aimed to present a simplified approach to be applied at a design stage in order to help to obtain an optimized TCC floor solution in terms of mechanical behavior and expenses. Therefore, an experimental set of results obtained from real-scale TCC floors tested under concentrated loads, together with the results of a parametric study using a Finite Element Method (FEM) model developed and validated by the authors was proposed.

## 2. Parametric Study

To achieve the set goal, a comprehensive parametric study was developed. Aiming at studying the mechanical behavior of medium span TCC floors (4.00 m), a Base Simulation (BS) was established. The BS composite slab has a square plan and is composed of a 0.07 m-thick concrete layer, seven timber beams 0.60 m apart from each other and a 0.02 m-thick timber interlayer. Its material and geometric characteristics can be found in Monteiro et al. [23]. To perform such a study, several parameters (Table 1) were chosen and their effect on the load distribution of TCC floors was analyzed. Only the loading of four beams, *B1* (end beam) to *B4* (central beam) was considered due to symmetry (for detailed information, see Monteiro et al. [23]). The analysis was accomplished by evaluating the percentage of support reaction (*sr*) received by each beam for the various loading cases: each beam loaded at a time, with a point load at  $1/2$  span or  $1/4$  span, or line load. Moreover, the distribution of vertical displacements (*vd*) at mid-span and the distribution of longitudinal bending moment at mid-span (*bm*) were analyzed.

Figure 1 summarizes the percentages of load received by the end beam (*B1* or *B7*) and the central beam when loaded, at a time, associated with BS, in terms of the analyzed quantities. Regardless of the loading case or location, the loaded beam does not receive the entire load but a share of it, as well as the unloaded beams, which emphasizes the existence of load distribution. The share of load received by the loaded beam will be higher or lower the farther or nearer that beam is from the center of the slab, respectively. Beam *B1* is the one associated with the highest share of load when loaded (more than 80% for *sr*). In addition, when considering the extreme load locations, *B1* vs. *B4*, the maximum deviation of received share is associated with this beam location (difference between the percentage of load associated with *B1* when the load is applied at *B1* and the percentage of load associated with *B1* when the load is applied at *B4* is about 90% for *sr*, for the three loading cases under consideration). On the contrary, intermediate beams show smaller deviations, with *B3* presenting the minimum deviation (difference between the percentage of load associated with *B3* when the load is applied at *B1* and the percentage of load associated with *B3* when the load is applied at *B4* is about 20% for *vd* and *bm*, for  $1/2 Pt$  and  $Ln$ , reaching less than 5% for  $1/4 Pt$ ).

Concerning the studied parameters, it was found that they affect in different amounts the quantities analyzed. The ones with a greater effect (more than 10% of deviation) are displayed in Tables 2–4. The deviation was computed between two modeling tasks associated with a parameter. The *Details* column specifies among which “parameter values” was the maximum deviation obtained (e.g., a maximum deviation of 75% was found among BS with two different support conditions (*Ss* vs. *Sae*) when loaded with a point load at mid-span of *B1*).

**Table 1.** Parameters studied.

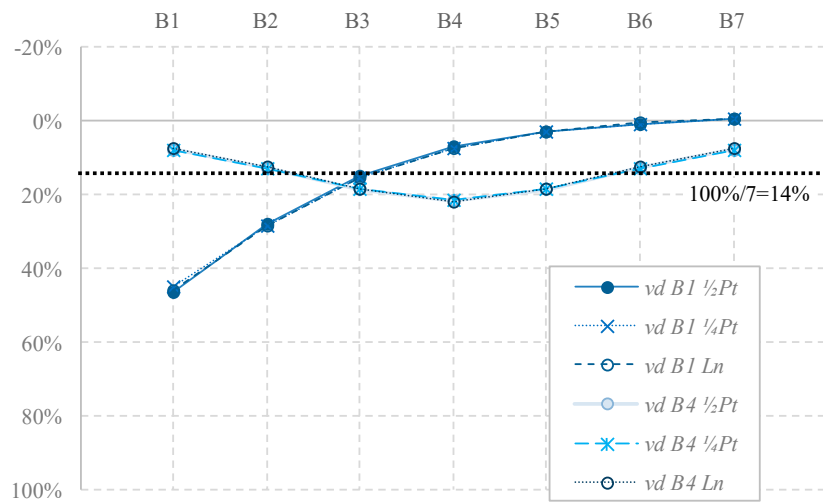
Type	Parameter		Symbol
Geometrical	Slab	Span	$L$
		Width	$b_{slab}$
		Beam spacing	$s_b$
	Cross-section	Thickness	Concrete Interlayer Timber
Shape		Beam	$\square, I, \circ$
Concrete		Strength class	According to EC2 [24]
	Aggregates	Normal-weight	NWAC
		Light-weight	LWAC
Material	Timber	Strength class	According to EN 338 [25]
		Product	Solid Wood-engineered
			GL, LVL, OSB + LVL, CLT
Mechanical behavior	Connection stiffness	Low	$IK$
		Medium	$mK$
		High	$hK$
	Material	Linear	Elastic
Non-linear		Elastic Perfectly-plastic	$EPP$
Support conditions, $Sc$	Beams' ends	Simply supported	$Ss$
		Fixed	$Fx$
	All ends	Simply supported	$Sae$
Loading	Type	Point load	Mid-span Quarter-span
			$1/2 Pt$ $1/4 Pt$
	Location	Linear load	$Ln$
		On each beam at a time	$B1, B2, \dots, B7$
Floor use	Domestic and residential activities		$A$
	Areas where people congregate, with possible physical activities.		According to EC1 [26] $C4$
Degree of oversizing, $DO$	Timber cross-section	Undersized	$Un$
		EC5 "tight-fit"	According to EC5 [15] $EC5$
		Oversized	$Ov$

With: GL—Glued laminated timber; LVL—Laminated veneer lumber; OSB—Oriented strand board; CLT—Cross-laminated timber.

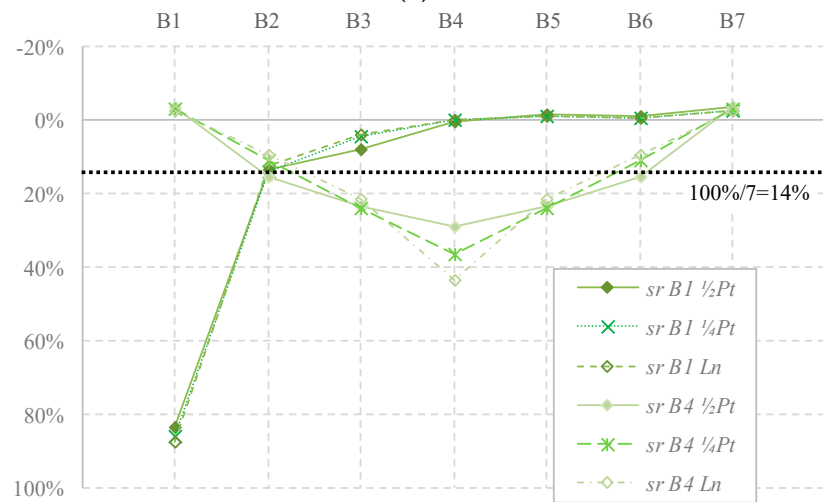
**Table 2.** Parameters with the greatest effect on the load distribution referring to BS.

Maximum Deviation [%]	Beam	Load Type	Quantity	Parameter	Details
75	$B1$	$1/2 Pt$	$sr$	Support conditions, $Sc$	Simply supported on beams' ends, $Ss$ vs. Simply supported on all ends, $Sae$
36	$B1$	$Ln$	$bm$		
31	$B1$	$Ln$	$vd$	Concrete thickness, $h_c$	0.02 m vs. 0.07 m (BS)
	$B2$	$1/2 Pt$	$sr$		
	$B1$	$Ln$	$bm$		
28	$B2$	$Ln$	$sr$	Span, $L$	4.00 m (BS) vs. 16.00 m *
27	$B1$	$1/2 Pt$	$sr$	Beams vs. deck	BS vs. CLT deck
26	$B1$	$1/2 Pt$	$vd$	Span, $L$	4.00 m (BS) vs. 16.00 m *
24	$B1$	$1/2 Pt$	$bm$		
17	$B1$	$Ln$	$vd$	Concrete strength	LC16/18 vs. C25/30 (BS)
16	$B1$	$Ln$	$bm$		
14	$B4$	$1/2 Pt$	$bm$	Beams vs. deck	BS vs. CLT deck
	$B2$	$Ln$	$sr$	Concrete strength	LC16/18 vs. C25/30 (BS)
10	$B1$	$1/2 Pt$	$vd$	Support conditions, $Sc$	Simply supported, $Ss$ vs. Fixed, $Fx$

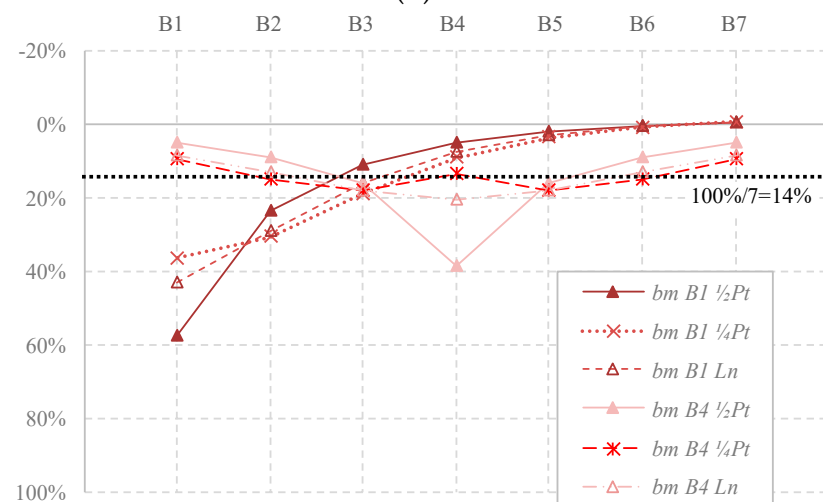
\*—underestimated timber section.



(a)



(b)



(c)

**Figure 1.** Percentage of load received by each beam when B1 or B4 is loaded, in terms of (a) *vd*; (b) *sr*; and (c) *bm*.

**Table 3.** Parameters with the greatest effect on the load distribution, referring to the boundaries of each parameter.

Maximum Deviation [%]	Beam	Load Type	Quantity	Parameter	Details
70	B1	1/2 Pt	sr	CLT and Sc	CLT + Ss vs. CLT + Sae
58	-	1/2 Pt	sr	Load location	B1 vs. B4 for BS with IK connection
47	B2	Ln	sr	Span, L	2.00 m (BS) vs. 16.00 m*
45	B1	1/2 Pt	vd	Concrete thickness, $h_c$	0.02 m vs. 0.20 m
	B1	Ln	bm		
44	B1	Ln	vd	Span, L	2.00 m (BS) vs. 16.00 m*
43	B2	Ln	sr	$h_c$	0.02 m vs. 0.20 m
41	B1	Ln	bm	Span, L	2.00 m (BS) vs. 16.00 m*
32	B1	1/2 Pt	sr	CLT and $s_b$	BS + juxtaposed beams vs. CLT deck
29	-	Ln	vd	Load location	B1 vs. B4 for BS with LC16/18 concrete
		Ln	bm		
26	B1	Ln	vd	CLT and Sc	CLT + Ss vs. CLT + Sae
23	B1	1/2 Pt	bm		
18	B1	Ln	vd	Concrete strength	LC16/18 vs. C40/50
17	B1	Ln	bm		
15	B2	Ln	sr		
11	B1	Ln	vd	CLT and $s_b$	BS + juxtaposed beams vs. CLT deck
	B1	Ln	bm	CLT and $s_b$	

\*—underestimated timber section.

**Table 4.** Maximum deviation of load distribution associated with the DO.

Maximum Deviation [%]	Beam	Load Type	Quantity	Parameter	Details
60	-	1/2 Pt	sr	Load location	B1 vs. B4 for Un with L = 16.00 m
43	B1	Ln	vd	EC5	L = 4.00 m vs. L = 16.00 m
42	B1	Ln	vd	Ov	
41	B1	Ln	bm	EC5	
39	B4	Ln	sr	Un	
38	B1	1/2 Pt	vd	Un	
	B1	Ln	bm	Ov	
37	B1	Ln	bm	Un	L = 2.00 m vs. L = 16.00 m
36	B2	Ln	sr	EC5	
31	B2	Ln	sr	Ov	
30	-	vd	Ln	Load location	
		bm	Ln		
66	B1	Ln	vd	Ov	L = 2.00 m vs. L = 16.00 m
64	B1	Ln	bm	Ov	
58	B1	Ln	vd	Un	
56	B1	1/2 Pt	vd	EC5	
	B1	Ln	bm	Un	
	B2	Ln	sr	Un	
	B2	1/2 Pt	sr	EC5	
	B2	1/2 Pt	sr	Ov	
53	B2	1/2 Pt	sr	EC5	

From this analysis, it becomes clear the significant effect of the following parameters:

1. The support conditions, with a maximum deviation of 75% between BS (Ss) and BS with Sae);
2. The degree of oversizing, with a maximum deviation of 66% (Ov), 58% (Un) and 56% (EC5), considering the limit spans 2.00 m and 16.00 m;

3. The loading position, with a maximum deviation of 58% considering the loading applied at B1 vs. applied at B4 when the modeling BS with IK connection is considered (reaching 60% when in association with DO—verified for the modeling task with the same cross-section as BS and  $L = 16.00$  m (underestimated timber section));
4. The span length, with a maximum deviation of 47% between spans of 2.00 m and 16.00 m;
5. The concrete thickness, with a maximum deviation of 45% between thicknesses of 0.02 m and 0.20 m;
6. The existence of a timber deck underneath the concrete layer, instead of timber beams and interlayer using juxtaposed beams or a CLT deck, with a maximum deviation of 27%; and
7. The concrete strength, with a maximum deviation of 18% between an LWAC LC16/18 and an NWAC C40/50.

Although the *DO* has shown a great effect, both *Ov* and *Un* series, varying between 31% (*sr*) and 42% (*vd*) when considering spans of 4.00 m (the same as BS) and 16.00 m (reaching deviations of 66% and 58% when considering the extreme spans [2.00 m; 16.00 m]), the percentages found are only indicative of the trend. In contrast, for the *EC5* series, the sections found were established based on an objective criterion: the design based on Annex B of EC5 [15], aiming at maximizing the section strength utilization ratio, for *Un* and *Ov* series that did not occur. Although a common procedure has been established, by changing only the timber height, no uniform percentage of over or under sizing was defined (for extra detail see Monteiro et al. [23]).

The analysis of the previous tables shows that most of the parameters that have the greatest effect on the load distribution are associated with the end beam *B1* (or *B7*). This was verified in 71% of the cases when considering the variation relatively to BS; 78% of the cases, when considering the variation of a parameter (except *DO*) among its extreme values; and in 67% of the cases, when considering the variation on the *DO*, as for  $L = [4.00 \text{ m}; 16.00 \text{ m}]$ , as for  $L = [2.00 \text{ m}; 16.00 \text{ m}]$ . This is due to the fact that end beams tend to concentrate the load applied over it (and thus, a lower percentage of distributed load) when compared with the remaining ones, allowing a higher variation than the central beam (*B4*), for instance, where the opposite happens, and a smaller range of variation can occur. With regard to the loading, although most of the listed parameters were associated with a linear loading, the differences found relatively to a point load at mid-span were, at most, 4% (disregarding the *Sc* modeling task, which, due to a different structural system, were associated with greater differences).

### 3. Simplified Approach

The design stage is a crucial stage where the designer must be able to come up with an economical structural solution, preferably in the shortest time possible. Knowing the percentage of load received by a specific beam, before the floor being built, without the need to numerically modeling it, will surely contribute to it. Thus, based on the findings of the parametric study and aiming at providing a practical tool capable to predict the sought percentage, a simplified equation was developed.

As shown above, three quantities were used for evaluating the load distribution, *vd*, *sr* and *bm*, but only one was used on the simplified model: the longitudinal bending moment, given its importance in the design process. For that, three essential parameters were considered: the span length, the concrete thickness and the transversal location of the beam. For this last consideration, a dimensionless parameter designated “beam location”, *bl*, was defined in order to provide the transversal position of the beam in question, relatively to the longitudinal axis of the outermost beam (*B1*) (Figure 2).

The results collected in the parametric study, specifically, the percentage of load received by the loaded beam for the three parameters listed above were treated and gathered. Four sets of “continuous” curves were obtained, based on the design considerations, BS, *EC5*, and *ov*, for the considered loadings, gathering the results for *B1* to *B4*, for each loading by span. Various polynomial approaches to the BS curves were tried in the approximation process: from a first-degree polynomial simple Equation

(1) to a fourth-degree polynomial simple Equation (3), considering also first (2) and second-degree polynomial equations with crossed terms).

$$z = a_0 + a_1 \cdot x_1 + a_2 \cdot x_2 + a_3 \cdot x_3, \quad (1)$$

$$z = a_0 + a_1 \cdot x_1 + a_2 \cdot x_2 + a_3 \cdot x_3 + a_4 \cdot x_1 \cdot x_2 + a_5 \cdot x_1 \cdot x_3 + a_6 \cdot x_2 \cdot x_3, \quad (2)$$

$$z = a_0 + a_1 \cdot x_1 + a_2 \cdot x_2 + a_3 \cdot x_3 + a_4 \cdot x_1^2 + a_5 \cdot x_2^2 + a_6 \cdot x_3^2 + a_7 \cdot x_1^3 + a_8 \cdot x_2^3 + a_9 \cdot x_3^3 + a_{10} \cdot x_1^4 + a_{11} \cdot x_2^4 + a_{12} \cdot x_3^4, \quad (3)$$

where  $x_1$ —span length;  $x_2$ —beam location;  $x_3$ —concrete thickness; and  $a_i$ , with  $i = 0$  to 12—polynomial coefficients.

The attempt to obtain the best approximation with the various polynomial equation was made by obtaining a set of polynomial coefficients, according to the polynomial under consideration through the minimization of the sum of the squared differences between the numerical and the polynomial predictions. To measure the “strength of the approximation”, the determination coefficient,  $R^2$ , (4) was used, for which the strongest approximation corresponds to  $R^2 = 1$  and the weakest approximation to  $R^2 = 0$ . Detailed information about the coefficients obtained for the various sets and loading cases, together with the corresponding  $R^2$ , can be found in Monteiro [27].

$$R^2 = \frac{\sum (z_i - \bar{z})^2}{\sum (Z_i - \bar{z})^2}, \quad (4)$$

where  $R$ —correlation coefficient,  $z_i$ —value given by the polynomial fit for the  $i$  point, location,  $\bar{z}$ —average of the values to approximate,  $Z_i$ —value to approximate for the  $i$  point, location.

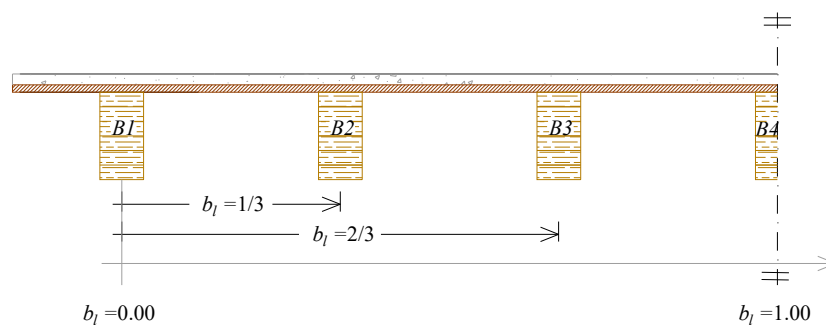


Figure 2. Beam location parameter.

Since the goal was to obtain an equation to predict the behavior of TCC floors under concentrated loads, the polynomial coefficients obtained for the various attempts were analyzed aiming at finding common tendencies among them, for different loadings. Given that the BS set was the only one for which three loading cases,  $1/2 Pt$ ,  $1/4 Pt$ , and  $Ln$ , were modeled (for the remaining sets only  $1/2 Pt$  and  $Ln$  were modeled); this was the chosen set to perform that comparison. The polynomial coefficients for all attempts for BS were compared with each other and among the various loading cases ( $1/2 Pt$  vs.  $Ln$ ;  $1/4 Pt$  vs.  $1/2 Pt$ ;  $1/4 Pt$  vs.  $Ln$ ). This analysis evidenced similar coefficients for comparable polynomial attempts and among those the one with the best approximation was identified: the second-degree polynomial simple equation. The polynomial coefficients of the sought equation, designated  $Pr$  (since it intends to predict the percentage of load received by the loaded beam), were defined as the computed average polynomial coefficients found for the three loading cases (5). Figure 3 shows its course as a function of the floor span. As the figure depicts, some differences can be found between the predicted and the numerical percentages, with  $Pr$  approaching the  $Ln$  load case curve more than the other curves. In general, it tends to underestimate the percentage of load associated with  $1/2 Pt$ , but it tends to overestimate the same quantities concerning  $1/4 Pt$  and  $Ln$ . Although for both point loadings, the greatest deviation is about  $\pm 20\%$  (associated, essentially, with the thinner concrete layers), the mean

differences were rather lower: about  $-11\%$  for  $1/2 Pt$  and  $+8\%$   $1/4 Pt$ . For  $Ln$  the deviations are lower than the point loadings, ranging between  $-10\%$  and  $+15\%$ , with a mean difference of  $+4\%$ .

$$Pr = 0.90 - 0.05 \cdot x_1 - 0.472 \cdot x_2 - 4.696 \cdot x_3 + 0.002 \cdot x_1^2 + 0.299 \cdot x_2^2 + 15.805 \cdot x_3^2, \quad (5)$$

where  $x_1$ —span length;  $x_2$ —beam location; and  $x_3$ —concrete thickness.

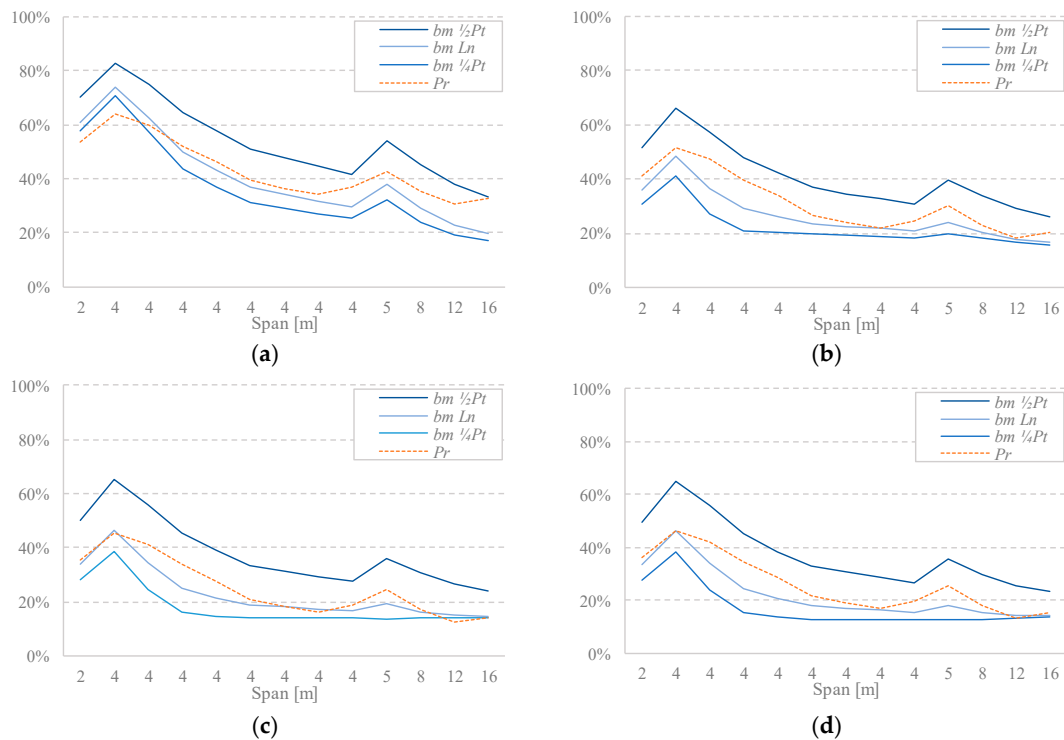


**Figure 3.** Percentage of  $bm$  received by the loaded beam (a) B1; (b) B2; (c) B3, and (d) B4 of BS set for the various loadings and  $x_i$ .

For evaluating its adequacy to predict the load distribution also in terms of  $vd$  and  $sr$ , percentages obtained with  $Pr$  were compared with the experimental results of five real-scale TCC floors' specimens, built and experimentally tested by the authors, subjected to point and line loads at different locations (S1, S2, S3, S4 and S5 differing between them essentially in terms of concrete strength and thickness, and span) [16]. Experimental vertical displacements, at mid- and quarter-span ( $vd \ 1/2 L$  and  $vd \ 1/4 L$ , respectively) and support reactions were recorded and worked in order to obtain the corresponding percentage. By comparing the experimental and  $Pr$  percentage curves, a similar course was found; however, differences were relatively high in some cases (mainly associated with  $sr$ —when computing the difference between the percentage obtained with  $Pr$  (independent of the loading type) and the experimental percentage for a specific beam, loading type, and loading location, the values range between  $-4\%$  and  $-42\%$ , with a maximum average partial difference  $-28\%$ , concerning a medium span floor (4.00 m) using NWAC, as has S1. In order to make simplified approach suitable to predict the percentage of load received by the loaded beam, regarding the three quantities,  $vd$ ,  $sr$  and  $bm$ , an extra coefficient was defined,  $cf_i$  with  $i = \{vd, sr, bm\} = \{1.25, 1.60, 1.00\}$ , for which  $Pr$  was multiplied. Figure 4 presents a good agreement between experimental and  $Pr \cdot cf_{vd}$  curves. This is also proven by the decrease of the average partial differences computed between the percentages obtained with  $Pr \cdot cf_i$ , with  $i = \{vd, sr, bm\}$  and experimental ones (Table 5). The extreme values varied from  $-7\%$  to  $8\%$  for  $vd \ 1/2 L$ ,  $-9\%$  and  $6\%$  for  $vd \ 1/4 L$ , and from  $-14\%$  to  $19\%$  for  $sr$  (with a maximum average partial difference of  $11\%$  for the S1 experimental specimen). Thus, concerning the specimen with average span dimensions (4.00 m) and regular materials specifically concrete (NWAC), S1, a slightly overestimated

prediction was obtained with the simplified approach, with a predicted percentage of load higher than that obtained experimentally.

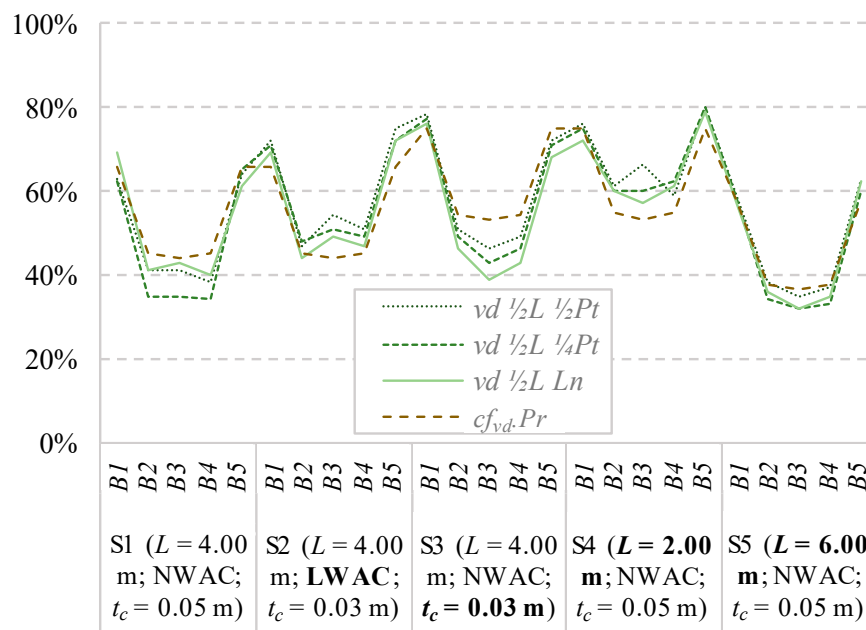


Figure 4. Percentage of  $vd \frac{1}{2} L$  received by the loaded beam for floors S1 to S5, for the various loadings.

Table 5. Average partial differences for the three loadings [%].

$Pr \cdot cf_i$	Quantity vs.	$vd \frac{1}{2} L$			$vd \frac{1}{4} L$			$sr$		
		$\frac{1}{2} L$	$\frac{1}{4} L$	$Ln$	$\frac{1}{2} L$	$\frac{1}{4} L$	$Ln$	$\frac{1}{2} L$	$\frac{1}{4} L$	$Ln$
Experimental specimen	S1 ( $L = 4.00$ m; NWAC; $t_c = 0.05$ m)	4	7	2	4	3	1	11	6	-2
	S2 ( $L = 4.00$ m; LWAC; $t_c = 0.05$ m)	-7	-5	-3	-5	-9	-4	3	-6	-14
	S3 ( $L = 4.00$ m; NWAC; $t_c = 0.03$ m)	3	5	8	6	1	6	19	9	-1
	S4 ( $L = 2.00$ m; NWAC; $t_c = 0.05$ m)	-6	-5	-3	-3	-4	-2	-3	-8	-9
	S5 ( $L = 6.00$ m; NWAC; $t_c = 0.05$ m)	-1	2	1	0	-3	-1	4	0	-5

#### 4. Conclusions

Concentrated loads are common loads in building floors, a consequence of heavy furniture or partition walls. The usual design of TCC floors considers the entire load associated with the loaded beam. However, this may be far from reality, more so if the loaded beam is nearer to the floor center (mid-width). That assumption may lead to overestimated sections, which will be consequently uneconomic and, at the same time, detrimental concerning the load distribution. An extensive parametric study developed using Finite Element (FE) numerical models was performed and the parameters that most affect the distribution of concentrated loads in the transverse direction were identified. The floor’s support conditions, the degree of oversizing, the loaded beam, the span length, the concrete thickness, the structural system (deck vs. timber beams underneath the concrete layer) and the concrete strength were the parameters that showed the highest effect. The goal of this study was to obtain a simplified approach capable of predicting the behavior of TCC floors subjected to a concentrated load, which could be applied at the design stage. Thus, a polynomial equation that can predict the percentage of load received by the loaded beam based on the floor span, the concrete thickness, and beam location, in terms of vertical displacement, support reactions and longitudinal bending moment was devised. Compared with the results of real-scale floor specimens, the simplified approach leads to differences usually small (<10%) and “safe”, as the prediction tends to be higher than the experimental value. Nevertheless, this equation is not yet in its simplest form as the authors

would like. Therefore, further studies are ongoing to deepen the subject with the hope that in the near future, designers may easily use the simplified approach.

**Author Contributions:** A.D., S.M. and S.L. have read and agree to the published version of the manuscript. A.D. and S.M. conceived the studied issue; S.M. performed the experimental tests, developed the numerical model, performed the modelling tasks, analyzed the data and wrote the paper; A.D. and S.L. wrote the paper. All authors have read and agreed to the published version of the manuscript.

**Funding:** This research was funded by the Operational Program Competitiveness and Internationalization R&D Projects Companies in Co-promotion, Portugal 2020, within the scope of the project OptimizedWood–POCI-01-0247-FEDER-017867.

**Acknowledgments:** The authors would like to thank the ISISE-Institute for Sustainability and Innovation in Structural Engineering.

**Conflicts of Interest:** The authors declare no conflict of interest.

## Abbreviation

$bm$	is the longitudinal bending moment at mid-span
BS	is the Base Simulation
$b_{slab}$	is the width of the slab
CLT	is the Cross Laminated Timber
$cf_i$	is the extra coefficient to obtain a better approximation with $i = \{vd, sr, bm\}$
EPP	is the elastic-perfectly plastic behavior
$Fx$	is the fixed support condition
GL	is the Glued Laminated Timber, Glulam
$h_c$	is the concrete thickness
$h_i$	is the interlayer thickness
$hK$	is the high stiffness
$h_t$	is the height of the timber beam
$I$	is the I-shape cross-section
$L$	is the span
LE	is the linear elastic behavior
$lK$	is the low stiffness
$Ln$	is the line load
LVL	is the Laminated Veneer Lumber
LWAC	is the lightweight aggregate concrete
$mK$	is the medium stiffness
NWAC	is the normal strength concrete
$ov$	is the overestimated sizing section
$Pr$	designation of the simplified approach
$Pt$	is the point load
$R$	is the correlation coefficient
$Sae$	is the simply supported condition in all ends
$sb$	is the beam spacing
$Sc$	is the support condition
$sr$	is the support reaction
$Ss$	is the simply supported condition
$sw$	is the self-weight
$Un$	is the underestimated sizing section
$vd$	is the vertical displacement at mid-span
$\bar{Z}$	is the average of the values to approximate
$z_i$	is the value obtained by the polynomial fit for the $i$ point, location,
$Z_i$	is the value to approximate for the $i$ point, location.
□	is the rectangular shape cross-section
○	is the round shape cross-section

## References

1. Emperger, F. Der Holzbeton. *Dinglers Polytech. J.* **1920**, *335*, 109–112.
2. Dias, A.; Skinner, J.; Crews, K.; Tannert, T. Timber-concrete-composites increasing the use of timber in construction. *Eur. J. Wood Wood Prod.* **2016**, *74*, 443–451. [[CrossRef](#)]
3. Van Der Linden, M. Timber Concrete Composite Floor Systems. Ph.D. Thesis, University of Delft, Delft, The Netherlands, December 1999. Available online: <https://repository.tudelft.nl/islandora/object/uuid:6b2807c2-258b-45b0-bb83-31c7c3d8b6cd?collection=research> (accessed on 12 June 2019).
4. Jorge, L.; Lopes, S.; Cruz, H. Interlayer Influence on Timber-LWAC Composite Structures with Screw Connections. *J. Struct. Eng.* **2011**, *137*, 618–624. [[CrossRef](#)]
5. Yeoh, D. Behaviour and Design of Timber-Concrete Composite Floor System. Ph.D. Thesis, University of Canterbury, Christchurch, New Zealand, 2010. Available online: <https://ir.canterbury.ac.nz/handle/10092/4428> (accessed on 12 June 2019).
6. Lukaszewska, E. *Development of Prefabricated Timber-Concrete Composite Floors*; Luleå University of Technology: Luleå, Sweden, 2009.
7. Wacker, J.; Dias, A.; Hosteng, T. Investigation of Early Timber-Concrete-Composite Bridges in the USA. In Proceedings of the 3rd International Conference on Timber Bridges, Skellefteå, Sweden, 26–29 June 2017.
8. Zhu, W.; Yang, H.; Liu, W.; Shi, B.; Ling, Z.; Tao, H. Experimental investigation on innovative connections for timber-concrete composite systems. *Constr. Build. Mater.* **2019**, *207*, 345–356. [[CrossRef](#)]
9. Yeoh, D.; Fragiaco, M.; De Franceschi, M.; Heng Boon, K. State of the Art on Timber-Concrete Composite Structures: Literature Review. *J. Struct. Eng.* **2011**, *137*, 1085–1095. [[CrossRef](#)]
10. Branco, J.M.; Descamps, T.; Tsakanika, E. Repair and Strengthening of Traditional Timber Roof and Floor Structures. In *Strengthening and Retrofitting of Existing Structures*; Costa, A., Arêde, A., Varum, H., Eds.; Springer: Singapore, 2018; pp. 113–138.
11. Croatto, G.; Turrini, U. Restoration of historical timber structures—Criteria, innovative solutions and case studies. In Proceedings of the Intervir em Construções Existentes de Madeira, Guimarães, Portugal, 5 June 2014; Lourenço, B.P., Sousa, J.B.M.H.S., Eds.; Universidade do Minho: Braga, Portugal, 2014; pp. 119–136.
12. Projetos, Miguel Guedes Arquitectos, Lda. Available online: <http://www.miguelguedes.pt/pt/projetos/ver/palacio-do-raio-centro-interpretativo-de-memorias-da-misericordia/> (accessed on 12 June 2019).
13. Vencedores, 2016, Reabilitação do Palácio do Raio, in Prémio Nacional de Reabilitação Urbana. Available online: <https://premio.vidaimobiliaria.com/> (accessed on 12 June 2019).
14. Dias, A.; Fragiaco, M.; Gramatikov, K.; Kreis, B.; Kupferle, F.; Monteiro, S.; Sandanus, J.; Schänzlin, J.; Schober, K.; Sebastian, W.; et al. *Design of Timber-Concrete Composite Structures. A State-of-the-Art Report by COST Action FP1402/WG 4*; Dias, A., Schänzlin, J., Dietsch, P., Eds.; Verlag: Aachen, Germany, 2018. [[CrossRef](#)]
15. EU. *Eurocode 5: Design of Timber Structures—Part. 1–1: General—Common Rules and Rules for Buildings*; EN1995-1-1; European Committee for Standardization: Brussels, Belgium, 2004.
16. Monteiro, S.; Dias, A.; Lopes, S. Transverse distribution of internal forces in timber-concrete floors under external point and line loads. *Constr. Build. Mater.* **2016**, *102*, 1049–1059. [[CrossRef](#)]
17. Monteiro, S.; Dias, A.; Lopes, S. New guidelines for design of timber-concrete systems for point and line loads. In Proceedings of the WCTE 2016—World Conference on Timber Engineering, Vienna, Austria, 22–25 August 2016.
18. Dias, A.; Monteiro, S.; Martins, C. Reinforcement of timber floors—Transversal load distribution on timber-concrete systems. *Adv. Mater. Res.* **2013**, *778*, 657–664. [[CrossRef](#)]
19. Kieslich, H.; Holschemacher, K. Investigations on load sharing effects in timber-concrete composite constructions. In Proceedings of the 9th International Conference on Structural Analysis of Historical Constructions (SAHC 2014), Mexico City, Mexico, 14–17 October 2014; Peña, F., Chávez, M., Eds.; 2014. Available online: <https://www.semanticscholar.org/paper/INVESTIGATIONS-ON-LOAD-SHARING-EFFECTS-IN-COMPOSITE-KieslichHolschemacher/ffe798847d3b910f0f9266072092c4a7b3b7752a> (accessed on 12 June 2019).
20. Kieslich, H.; Holschemacher, K. Transversal load sharing in timber-concrete floors—Experimental and numerical investigations. In Proceedings of the 14 World Conference on Timber Engineering, Vienna, Austria, 22–25 August 2016.

21. Mudie, J.; Sebastian, W.M.; Norman, J.; Bond, I.P. Experimental study of moment sharing in multi-joist timber-concrete composite floors from zero load up to failure. *Constr. Build. Mater.* **2019**, *225*, 956–971. [[CrossRef](#)]
22. Antunes, S. Distribuição Transversal de Cargas em Lajes Mistas Madeira-Betão, Estudo da Influência da Secção Transversal. Master's Thesis, University of Coimbra, Coimbra, Portugal, 2019.
23. Monteiro, S.; Dias, A.; Lopes, S. Transverse distribution of concentrated loads in timber-concrete floors—Parametric study. *Proc. Inst. Civil Eng. Struct. Build.* in press. [[CrossRef](#)]
24. EU. *Eurocode 2: Design of Concrete Structures—Part. 1–1: General—Common Rules and Rules for Buildings*; EN1992-1-1; CEN: Brussels, Belgium, 2004.
25. EU. *Structural Timber*; EN338; European Committee for Standardization: Brussels, Belgium, 2003.
26. EU. *Eurocode 1: Actions on Structures—Part. 1–1: General Actions—Densities, Self-Weight, Imposed Loads for Buildings*; EN1991-1-1; European Committee for Standardization: Brussels, Belgium, 2001.
27. Monteiro, S. Load Distribution on Timber-Concrete Composite Floors. Ph.D. Thesis, University of Coimbra, Coimbra, Portugal, 2015.



© 2020 by the authors. Licensee MDPI, Basel, Switzerland. This article is an open access article distributed under the terms and conditions of the Creative Commons Attribution (CC BY) license (<http://creativecommons.org/licenses/by/4.0/>).